Phase Behavior of PS−PVME Nanocomposites

Koray Yurekli,[†] Alamgir Karim,[‡] Eric J. Amis,[‡] and Ramanan Krishnamoorti*[,†]

Department of Chemical Engineering, University of Houston, 4800 Calhoun, Houston, Texas 77204-4004, and Polymers Division, National Institute of Standards and Technology, Gaithersburg, Maryland 20899

Received April 7, 2003

ABSTRACT: The influence of nanometer thick, highly anisotropic organically modified layered silicate (montmorillonite) on the phase behavior of deuterated polystyrene (dPS) and poly(vinyl methyl ether) (PVME) is investigated by a combination of small-angle neutron scattering (SANS) and a two-dimensional combinatorial method based on light scattering and corroborated by single-point static cloud-point light scattering. The presence of layered silicates up to a volume fraction of 0.04 is found to leave the phase diagram essentially unchanged, with the values of the Flory−Huggins χ parameter at high temperatures being nearly independent of added silicate for blends with layered silicates up to a volume fraction of 0.008. These surprising results, in light of the significantly higher polarity of PVME in comparison to PS, allows us to investigate the influence of such layered silicates on the kinetics and morphology of phase separation in polymer blends as detailed in a previous paper.

Introduction

Polymer blends provide a convenient way of producing novel materials with properties different from, and often superior to, those of the constituent homopolymers. Frequently, fillers are used to further modify the mechanical, thermal, and barrier properties of these materials.[1] Research on the reinforcement of polymers by nanometer thick layered silicates studied in this work goes back to the late 1950s and early 1960s.[2] However, the first polymer−layered silicate nanocomposites with outstanding mechanical and thermal properties with added silicate volume fractions of only 0.02 that were used in commodity applications were developed by the Toyota research group in the early 1990s.[3]

The layered silicates belong to the class of 2:1 smectites.[2] These layers are roughly circular disks with effective diameters ranging from 30 nm to 10 μm and a thickness of ≈1 nm. Several layers are stacked into tactoids with the interlayer gallery (spacing on the order of a few nanometers) accommodating positive metal ions that balance the negative charge of the layers arising from the isomorphous substitution in the octahedral or tetrahedral sheets. Based on a density of 2200 kg/m^3 and a layer thickness of 1 nm, the surface area when fully delaminated or exfoliated is ≈800 m^2/g. The pristine silicate tactoids are hydrophilic due to the presence of the hydrated metal cations. For compatibility with the polymer, these metal cations are exchanged with organic cations that make the silicate hydrophobic.[2,4,5]

When nanoparticles are added to a polymer blend rather than a homopolymer, an additional concern is their effect on the thermodynamic phase behavior of the blend and on the morphology formed in the two-phase region. With the high surface areas associated with the layered silicates, it is expected that even small amounts of the nanofillers can have significant effects.[6] In fact, having such high surface area fillers in the system can be considered to be analogous to ultrathin films, where the phase behavior of blends is significantly different from bulk behavior even for the case of isotopic blends.[7] For example, in the case of a styrene−isoprene block copolymer, the addition of organically layered silicate at a volume fraction of 0.008 was found to change the order−disorder transition temperature by 6−30 K.[8] Recently, Lee and Han have shown a dramatic increase in the order−disorder transition temperature for a hydoxylated polystyrene−polyisoprene block copolymer mixed with an organically modified layered silicate.[9] Finally, significant decrease in domain sizes of strongly incompatible polymer blends by the addition of organically modified layered silicates have also been reported and suggest changes in either the thermodynamics or kinetics of phase separation.[10] Any changes to the phase-separated structures or the kinetics of their development are especially important because they can have a significant impact on the processing and properties of the material.

However, the effect of layered silicates on the thermodynamic phase behavior of a polymer blend must be examined first to form the basis for the examination of the morphological and kinetic consequences of such nanoparticle addition. In this study, the particular system chosen is a binary blend of deuterated polystyrene (dPS) and poly(vinyl methyl ether) (PVME), which has been studied extensively[11−14] and exhibits an accessible lower critical solution temperature (LCST) with a critical composition of PS volume fraction of 0.20 (nearly independent of molecular weight). A hydrophobically (dimethyl dioctadecylammonium) modified version of the naturally occurring layered silicate montmorillonite (2C18M) is used.

For the case of PS nanocomposites, Vaia and Giannelis[15] have demonstrated that the weak acid−base interactions between the polymer and silicate, resulting from the polar character of the silicates (even after organic modification)[16] and the weak polar components of interfacial energy of PS (dispersive solubility parameter, $\delta_d = 18.1$ MPa$^{1/2}$, and polar solubility parameter, $\delta_p = 1.1$ MPa$^{1/2}$),[17] leads to the development of intercalated nanocomposites. PVME, on the other hand, is

* To whom correspondence should be addressed. E-mail: Ramanan@uh.edu.
[†] University of Houston.
[‡] National Institute of Standards and Technology.

10.1021/ma0302098 CCC: $27.50
Published on Web 12/18/2003

significantly more polar. Based on group contribution calculations,[18] the dispersive component, δ_d, and the polar component, δ_p, for PVME have values of 15.5 and 7.1 $MPa^{1/2}$, respectively. In fact, PVME is known to intercalate even the pristine unmodified hydrophilic layered silicates.[2] Therefore, it is expected that the PVME will be preferentially attracted to the silicate surfaces, which might, based on the high surface area exposed to the polymer chains, lead to significant changes to the thermodynamics, kinetics, and morphology of phase separation for the blend even at relatively low volume fractions of added nanoparticle.

The phase behavior is examined using both small-angle neutron scattering (SANS) and a recently developed two-dimensional combinatorial method based on light scattering. Static cloud-point light scattering experiments are also performed to complement and verify the results from these methods.

Experimental Section

The dPS, obtained from Polymer Source,[19] has a weight average molecular weight (M_w) of 102 000 with a polydispersity (M_w/M_n) of 1.05.[20] The PVME has a M_w of 119 000 with a M_w/M_n of ≈2.5. The organically modified layered silicate is a previously characterized[21,22] dimethyl dioctadecylammonium substituted montmorillonite (2C18M), with a charge exchange capacity of 0.90 equiv/kg. Each individual silicate layer can be considered to be a disk with a thickness of 0.95 nm and diameter ranging from 0.5 to 1 μm.[23,24] The reported diameter of montmorillonite is a best estimate based on electron micrographs of a wide range of polymer nanocomposites that indicate the presence of a distribution of diameters that are thought to arise because of the edge−edge and edge−face aggregation, flexibility of the layers, and intrinsic inhomogeneity of these natural layered materials.[22,24]

The nanocomposites were prepared by solution mixing. The appropriate amounts of dPS and PVME were co-dissolved in toluene to get dPS volume fractions (ϕ_{dPS}) of 0.18, 0.28, and 0.58. Then, enough montmorillonite was added to result in a hybrid with 2C18M volume fractions of 0.004, 0.008, or 0.04. The resulting solution was allowed to dry in a fume hood. Once the bulk of the solvent was removed, the sample was placed in a vacuum oven for ≈10 h at room temperature followed by ≈6 h at ≈100 °C.

Small-angle neutron scattering (SANS) samples were prepared in the following way to achieve uniform, bubble-free samples: A brass washer with outer diameter of 25 mm, an inner diameter of 15 mm, and thickness of 1 mm was placed on a quartz window. Appropriate quantities of the blend were placed in the annulus of the brass washer and heated in a vacuum oven at a temperature of ≈130 °C. Once a bubble-free sample that filled the annulus completely was achieved, it was capped using a second quartz window. SANS measurements were performed on the 30-m SANS beamline (NG7) at NIST, Gaithersburg, MD. Neutrons with wavelength (λ) of 6 Å and $\Delta\lambda/\lambda$ of 0.15 were used with two different experimental arrangements with sample to detector distances of 4 and 12 m. The resulting q ranges were ≈(0.008−0.12) $Å^{-1}$ and (0.005−0.04) $Å^{-1}$, respectively. The SANS data were reduced and corrected for parasitic background and empty-cell scattering. Absolute cross sections were obtained with the use of a silica secondary standard for the 4-m configuration and a polystyrene isotopic blend standard for the 12-m configuration. Finally, a q-independent incoherent scattering correction, assumed to primarily originate from protons, was subtracted prior to data analysis. The incoherent scattering calculations were based on the scattering from a purely protonated PVME and the proton density of the studied samples. The coherent intensity was converted to the structure factor by accounting for the contrast factor.[12] The SANS based structure factor was interpreted in the context of the Flory−Huggins−Staverman lattice theory, which gives the Gibbs free energy of mixing per unit volume, ΔG_M, for a binary polymer blend as

$$\frac{\Delta G_M}{kT} = \frac{\phi_1}{N_1\left(\frac{v_1}{v_0}\right)}\ln \phi_1 + \frac{\phi_2}{N_2\left(\frac{v_2}{v_0}\right)}\ln \phi_2 + \chi\phi_1\phi_2 \qquad (1)$$

where k is the Boltzmann constant, v_i and N_i are the volume per repeat unit and the number of repeat units in a chain of component i, ϕ_i is the volume fraction of component i, and χ is the Flory−Huggins interaction parameter based on a reference volume of v_0.

For static cloud-point light scattering measurements, ≈0.03 g of sample was placed at the bottom of a glass tube and annealed at ≈120 °C for ≈4 h to form a uniform layer. The glass tubes were then filled with argon to prevent degradation during the experiments and sealed using a blowtorch. The light scattering measurements consisted of immersing the tubes in a temperature-controlled (via a resistance heater inside the oil bath connected to a variable voltage source) oil bath and determining the binodal for each sample by the onset of opacity. To aid the determination of opacity, a black line was drawn on the underside of each tube with a permanent marker and the visibility was monitored as a function of temperature. Layered silicate filled and pure blends of each blend composition were immersed simultaneously for consistency. Further, the unfilled blend measurements were repeated several times to determine the reproducibility of the method.

A combinatorial method to determine the entire phase diagram for the polymer blend as outlined by Meredith et al.[25,26] was used to produce the phase diagrams from films cast on hydrophobic Si wafers. The preparation of the sample and the experimental method to determine the phase diagram involve four steps. The first step, gradient mixing, starts with a pure PVME solution in a vial. Then, an inflow of dPS solution and an outflow of the mixed solution are started simultaneously. As a result, the composition of the blend changes as a function of time. A sampling syringe is used to continuously sample and store this gradient. In the second step, the gradient solution is deposited from the syringe on one edge of a Si wafer using a moving stage. Third, this gradient stripe is spread as a film by moving the wafer under a stationary knife. Finally a temperature gradient orthogonal to the composition gradient is applied under vacuum in order to perform a two-dimensional combinatorial experiment. Meredith and co-workers[25] have shown that disturbances to the concentration gradient through turbulence during sampling and through molecular diffusion during storage in the syringe are negligible. Further, according to Meredith and co-workers and other previous studies,[25,27] the minimum film thickness required for agreement with bulk measurements is ≈100 nm.

The composition range for the experiments described here, calculated from the flow rates that were used, was from a PVME mass fraction of 0.2 to 1.0. Previously, Meredith et al.[25] have shown that these calculations are consistent with the experimental measures of the composition using IR spectroscopy. The temperature gradient was from 115 to 190 °C for the unfilled blend and from 115 to 195 °C for the blend film containing a 2C18M volume fraction of 0.008. Film thicknesses were ≈1 μm, which implies that the phase behavior should be unchanged from bulk behavior.

Finally, X-ray diffraction (XRD) was performed on the nanocomposites of the individual homopolymers with 2C18M and the blend with 2C18M containing layered silicate volume fractions of 0.008 using a Siemens D5000 X-ray diffractometer[19] with Cu Kα radiation of 1.54 Å generated at 30 mA and 40 kV. Experiments were conducted over 2θ values ranging from 2° to 10° with intensities measured for 1 s at each 0.02-deg step.

Unless otherwise specified, all error values reported are 1 standard deviation and are taken as an estimate of the standard uncertainty.

Results and Discussion

The coherent SANS intensity as a function of temperature for a near-critical unfilled dPS/PVME (ϕ_{dPS} =

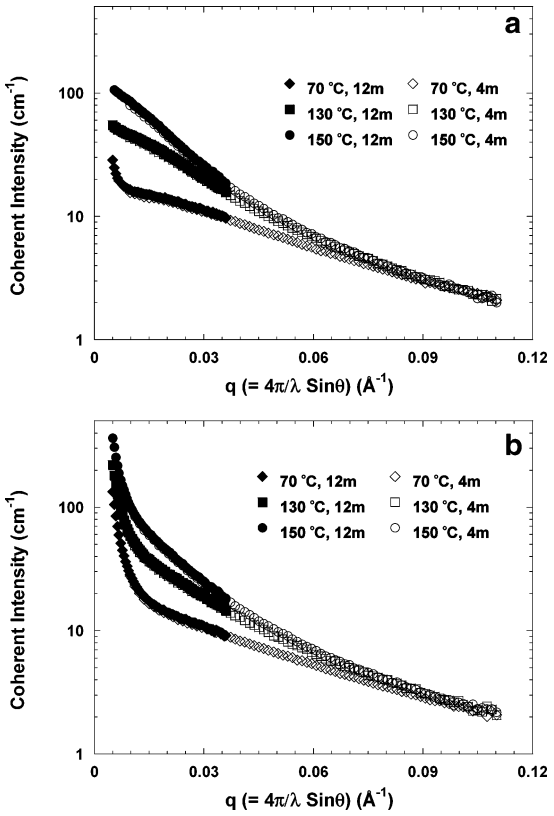

Figure 1. Coherent intensities from SANS for the pure $\phi_{dPS} = 0.28$ blend (a**)** and the $\phi_{dPS} = 0.28$ blend nanocomposite with a 2C18M volume fraction of 0.008 **(**b**)** at different temperatures. Each curve is a composite of data collected using the two instrumental setups detailed in the Experimental Section, allowing access to both high and low q values. For these curves and for all the curves in the following figures, the absence of error bars indicates that the standard deviation on the data is smaller than the marker size. As expected from an LCST system, higher temperatures lead to larger concentration fluctuations, resulting in higher intensities at low q values.

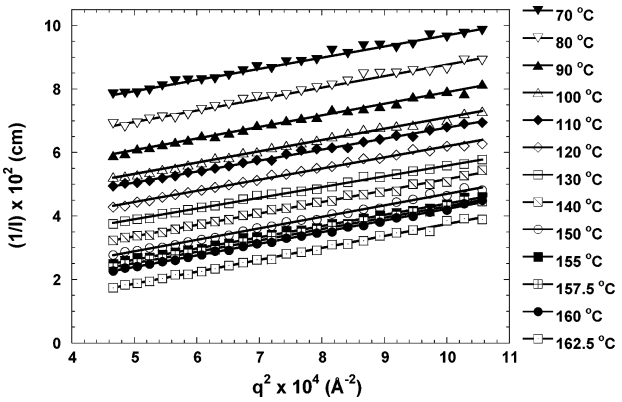

Figure 2. Inverse coherent intensity vs q squared curves for the nanocomposite of the $\phi_{dPS} = 0.28$ blend with a 2C18M volume fraction of 0.004 for all measured temperatures. The lines though the data are linear fits used to extrapolate the zero q intercepts.

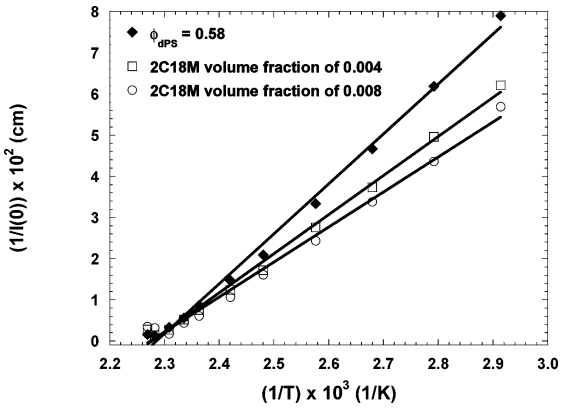

Figure 3. Extrapolated zero q inverse coherent intensities graphed against temperature for dPS/PVME blends and nanocomposites with $\phi_{dPS} = 0.58$. The presence of 2C18M at volume fractions of 0.004 or 0.008 seems to have little or no effect on the phase behavior of the polymer blend.

0.28) blend is shown in Figure 1a. The intensity increases at low q with increasing temperature and demonstrates the increased concentration fluctuations with increasing temperature, consistent with an LCST. The same trend is observed for the dPS/PVME ($\phi_{dPS} = 0.28$) blend with a 2C18M volume fraction of 0.004 as shown in Figure 1b. However, at low q, a significant upturn is present in the intensity at all temperatures and is attributed to the scattering from the aggregates of layered silicates corresponding to the intercalated structure.

On the basis of the Einstein−Smoluchowski equation and the incompressible Flory−Huggins theory (eq 1), the limit of stability for these binary blends of dPS and PVME were determined by examination of the temperature dependence of $I(0)$, the extrapolated coherent scattering intensity in the forward angle; i.e., $q = 0$. For a binary mixture, the coherent scattering at low q is adequately described by the Ornstein−Zerneike equation:

$$I(q) = \frac{I(0)}{1 + \xi^2 q^2} \tag{2}$$

where ξ is the correlation length. $I(0)$ values as a function of temperature can thus be estimated by extrapolating the $1/I(q)$ vs q^2 data to $q = 0$ as shown in Figure 2. For the $\phi_{dPS} = 0.58$ blend composition, only temperatures of 140 °C and higher are used to construct these extrapolations of the spinodal temperature. At lower temperatures concentration fluctuations in the blend are suppressed and the scattering from the layered silicate dominates. The minimum q value used is determined by calculating the contribution to the coherent scattering intensity from the layered silicate tactoids and ensuring that this contribution, as calculated from the fitting of the SANS curves described in the following section, is no more than 10% for the worst case for each blend composition, i.e., 70 °C for the sample containing a 2C18M volume fraction of 0.008. At higher loadings of the silicate, the scattering from the silicates dominates over the blend making it unreasonable to use SANS measurements to accurately determine thermodynamic behavior using this simplified approach.

The scattering in the forward angle, $I(0)$, at the limit of stability approaches infinity, with $I(0)$ in the single-phase region $\sim(\chi_s - \chi)^{-1}$, where χ_s is the Flory−Huggins interaction parameter at the spinodal (i.e., $\chi_s = 1/2(1/\phi_1 N_1(v_1/v_0) + 1/\phi_2 N_2(v_2/v_0))$). Moreover, the binodal, if distinct from the spinodal, can also be qualitatively recognized from a plot of $1/I(0)$ vs $1/T$, as a discontinuous deviation from the roughly straight-line behavior in the single-phase region. The $1/I(0)$ vs $1/T$ data for the $\phi_{dPS} = 0.58$ blend is shown in Figure 3 as a function of 2C18M concentration with estimates of the spinodal

Table 1. Spinodal Temperatures

2C18M concentration, vol fractn	$T_{spinodal} \pm 2$, °C		
	$\phi_{dPS} = 0.18$	$\phi_{dPS} = 0.28$	$\phi_{dPS} = 0.58$
0	161	164	167
0.004	156	172	167
0.008	159	169	165

from linear fits for all blend compositions shown in Table 1. The extrapolated spinodal temperatures for the different blend compositions are roughly similar, indicating a shallow phase diagram. For the $\phi_{dPS} = 0.18$ blend, the binodal point cannot be distinguished from the spinodal, while the $\phi_{dPS} = 0.58$ blend, which is farthest from the critical point, only shows a 3 °C difference between the observed binodal and the extrapolated spinodal, indicating a narrow metastable region. These observations are in good agreement with previous studies that have shown the PS−PVME phase diagrams to have weak composition dependence and a narrow metastable region except at highly off-critical concentrations.[11,28] Finally, the addition of 2C18M up to a volume fraction of 0.008 does not significantly alter the phase behavior of the blend. (SANS analysis results for the $\phi_{dPS} = 0.18$, 0.28, and 0.58 blends are given in Tables 2−4.)

A more quantitative examination of the phase behavior of the blend from the SANS data is obtained by fitting the q dependence of the scattered coherent intensity profile using the incompressible random phase approximation (RPA) model to obtain the Flory−Huggins interaction parameter, χ, between the two homopolymers. For a polymer blend with no added nanoparticles, the coherent scattered intensity is

$$I(q) = k_n S(q) \tag{3}$$

where $S(q)$ is the structure factor and k_n the scattering contrast factor. For the structure factor calculations, PS is considered as monodisperse, while PVME is assumed to have a Zimm-Shultz molecular weight distribution.

However, the RPA equation as written for a binary blend of homopolymers is not sufficient to model the layered silicate filled blend system. To account for the intraparticle scattering from the layered silicate, a form factor ($P(q)$) is introduced and the coherent scattered intensity modeled as

$$I(q) = k_n P(q) S(q) \tag{4}$$

$P(q)$ is chosen to be of the form $(1 + \beta q^{-3})$, with β being an adjustable prefactor, and provides a significant contribution at low q values that correspond to the length scale of the layered silicate tactoids and approaches one as q becomes large. The q^{-3} dependence

Table 2. SANS Analysis Results for the $\phi_{DPS} = 0.18$ Blends

	no 2C18M		2C18M vol fractn of 0.004		2C18M vol fractn of 0.008	
T, °C	χ	100(1/I(0)), cm	χ	100(1/I(0)), cm	χ	100(1/I(0)), cm
70	−0.0102	5.60	−0.0109	5.26	−0.0121	5.46
100	−0.0049	3.25	−0.0050	2.99	−0.0053	2.97
120	−0.0021	2.04	−0.0020	1.72	−0.0024	1.87
140	−0.0001	0.95	0.0004	0.80	0.0001	0.87
150	0.0010	0.56	0.0013	0.32	0.0010	0.48
155	0.0014	0.35	0.0017	0.18	0.0015	0.23
160	0.0018	0.19			0.0019	0.05

Table 3. SANS Analysis Results for the $\phi_{DPS} = 0.28$ Blends

	no 2C18M		2C18M vol fractn of 0.004		2C18M vol fractn of 0.008	
T, °C	χ	100(1/I(0)), cm	χ	100(1/I(0)), cm	χ	100(1/I(0)), cm
70	−0.0115	6.02	-0.0136	6.18	−0.0140	5.64
80	−0.0096	5.05	-0.0111	5.14	−0.0115	4.90
90	−0.0077	4.28	-0.0089	4.25	−0.0093	4.11
100	−0.0060	3.49	-0.0069	3.55	−0.0073	3.48
110	−0.0049	2.99	-0.0062	3.33	−0.0068	3.12
120	−0.0035	2.36	-0.0047	2.68	−0.0047	2.56
130	−0.0022	1.75	-0.0034	2.20	−0.0034	2.02
140	−0.0010	1.17	-0.0021	1.55	−0.0016	1.32
150	0.00004	0.77	-0.0010	1.07	−0.0005	0.83
155	0.0005	0.41	-0.0004	0.86	−0.0001	0.56
157.5	0.0008	0.33	-0.0001	0.73	0.0001	0.53
160	0.0009	0.26	0.0002	0.55	0.0004	0.37
162.5						

Table 4. SANS Analysis Results for the $\phi_{DPS} = 0.58$ Blends

	no 2C18M		2C18M vol fractn of 0.004		2C18M vol fractn of 0.008	
T, °C	χ	100(1/I(0)), cm	χ	100(1/I(0)), cm	χ	100(1/I(0)), cm
70	−0.0163		−0.0190		−0.0233	
85	−0.0120		−0.0135		−0.0159	
100	−0.0089		−0.0093		−0.0110	
115	−0.0057		−0.0064		−0.0071	
130	−0.0031		−0.0033		−0.0037	
140	−0.0017	1.47	−0.0018	1.24	−0.0022	1.06
150	−0.0005	0.86	−0.0006	0.75	−0.0011	0.61
155	0.0001	0.56	−0.0003	0.52	(0.0016)	0.44
160	0.0007	0.33	(0.0020)	0.27	(0.0023)	0.18
165	0.0015	0.13	(0.0025)	0.14		
167.5						

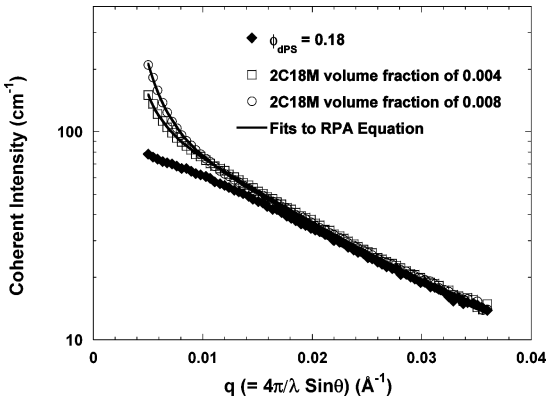

Figure 4. Fits of the 140 °C SANS data for the $\phi_{dPS} = 0.18$ blend containing varying amounts of 2C18M to the RPA equation modified for the intraparticle layered silicate scattering as described in the Results and Discussion. The quality of the fits is representative of all data except those collected close to phase separation.

is chosen in accordance with previous SANS studies of layered silicates dispersed in organic solvents. Ho et al.[29] and Hanley et al.[30] have shown that for organically modified montmorillonite in organic solvents, in the low-q region, a q^{-n} dependence is observed, where n is calculated to have a value of 2.1 for a single platelet, 2.36 for a two-platelet tactoid, and 2.9 for a 20-platelet tactoid.[29] For the intercalated nanocomposites studied here, tactoids with about five layers are estimated. Therefore, a value of three for n is reasonable for modeling the layered silicate contribution. This choice is also supported by recent SANS studies of intercalated PS and 2C18M.[31] Further, the actual fitting of the data only weakly depends on the value of n.

The scattering data were fit to the model given by eq 4 using l values of 6.8 Å for the dPS[12] and 5.8 Å for the PVME.[14] An adjustable prefactor α for the chain dimensions was used to account for any discrepancies resulting from using fixed l values obtained in previous SANS experiments. Values of α ranged from 0.97 to 1.03 for all temperatures and compositions examined here. Resulting fits to coherent SANS data for the $\phi_{dPS} = 0.18$ blend containing 2C18M volume fractions of 0, 0.004, and 0.008 at 140 °C are shown in Figure 4. The quality of these fits is representative except for the data sets at or near the spinodal temperature. The χ values for the unfilled and filled blends of all compositions are tabulated in Tables 2−4. For the higher temperature experiments of the $\phi_{dPS} = 0.58$ blend, it was not possible to achieve good RPA fits. Thus, the values in parentheses were calculated from $I(0)$ by using the modified Zimm model, i.e., the zero-angle extrapolated RPA equation:[12,32]

$$\frac{k_n}{I(0)} = \frac{1}{N_1 v_1 \phi_1} + \frac{1}{N_2 v_2 \phi_2} - 2\frac{\chi}{v_0} \qquad (5)$$

The values of $I(0)$ were obtained by extrapolating the scattering data to $q = 0$ using the O−Z formulation. Clearly, although χ depends on the 2C18M concentration at low temperatures, at high temperatures where concentration fluctuations are larger, the effect of added 2C18M becomes very small. These results are consistent with the $1/I(0)$ vs $1/T$ analysis presented above, which demonstrated that the extrapolated spinodal temperatures did not change appreciably with the addition of 2C18M up to a volume fraction of 0.008.

Table 5. Binodal Temperatures Determined from Light Scattering

2C18M concentration, vol fractn	$T_{binodal} \pm 2$ °C		
	$\phi_{dPS} = 0.18$	$\phi_{dPS} = 0.28$	$\phi_{dPS} = 0.58$
0	163	162	166
0.008		159	164
0.04		160	
0.04 2C18L[a]		160	

[a] 2C18L corresponds to a dimethyl dioctadecylammonium modified Laponite. Laponite is a synthetic layered silicate with a disk diameter of 30 nm and thickness 1 nm and a charge exchange capacity of 0.75 equiv/kg. Nanocomposites prepared of PS and PVME with 2C18L exhibit silent X-ray diffraction behavior suggesting poor ordering of the layers and possible exfoliation.

Because of the surprising SANS results, two light scattering methods were used to determine the phase boundaries. These experiments are sensitive to possible heterogeneities in the mixtures, particularly around the layered silicate particles. The results of the bulk cloud-point light scattering measurements are shown in Table 5 and are in reasonable agreement with those obtained from SANS.[33] We note that for the nanocomposites, the phase boundaries are quite sharp and phase separation occurs homogeneously (ranging from micrometers to millimeters) throughout the sample. Light scattering measurements were also performed for near critical blends with layered silicate volume fraction of 0.004 and the phase separation temperature was found to be unaffected. This concentration of layered silicate is significantly larger than the concentration of hydrodynamic overlap for exfoliated (i.e., a volume fraction of <0.01) and intercalated (i.e., a volume fraction of 0.02−0.025) hybrids. These results clearly suggest that, somewhat surprisingly, the thermodynamic interactions between PS and PVME are largely unaffected by the addition of the organically modified layered silicates.

A two-dimensional combinatorial phase behavior study was used to further corroborate the SANS and bulk light scattering measurements. Figure 5a is one such phase diagram recorded for a blend of dPS and PVME without any added layered silicate. The single-phase regions are transparent and show the dark background of the Si substrate. The phase-separated regions are white due to the difference in the refractive indices between the two phases and the resulting scattering of light. The temperature gradient was applied along the wafer edge coinciding with the y-axis, while the x-axis corresponds to the composition gradient. As a result, this method captures an entire phase diagram in a single experiment. Figure 5b is a similar phase diagram for the nanocomposite of dPS and PVME with a 2C18M volume fraction of 0.008. Consistent with the SANS and bulk light scattering, the combinatorial method clearly demonstrates that the addition of layered silicates results in essentially unaltered phase diagrams.

In Figure 5a, the phase boundaries are not well defined presumably due to the possible kinetic effects resulting in poor phase separation or dewetting of the polymer film associated with the phase separation of the polymer blend (at least at the intermediate or late stages as observed here). However, in Figure 5b the phase boundary is well-defined and suggests that the 2C18M either nucleates the phase separation or stabilizes the blend film on the Si substrate. Clearly, the nucleation and growth of the phases in the presence of the 2C18M influence the sharpness of the phase bound-

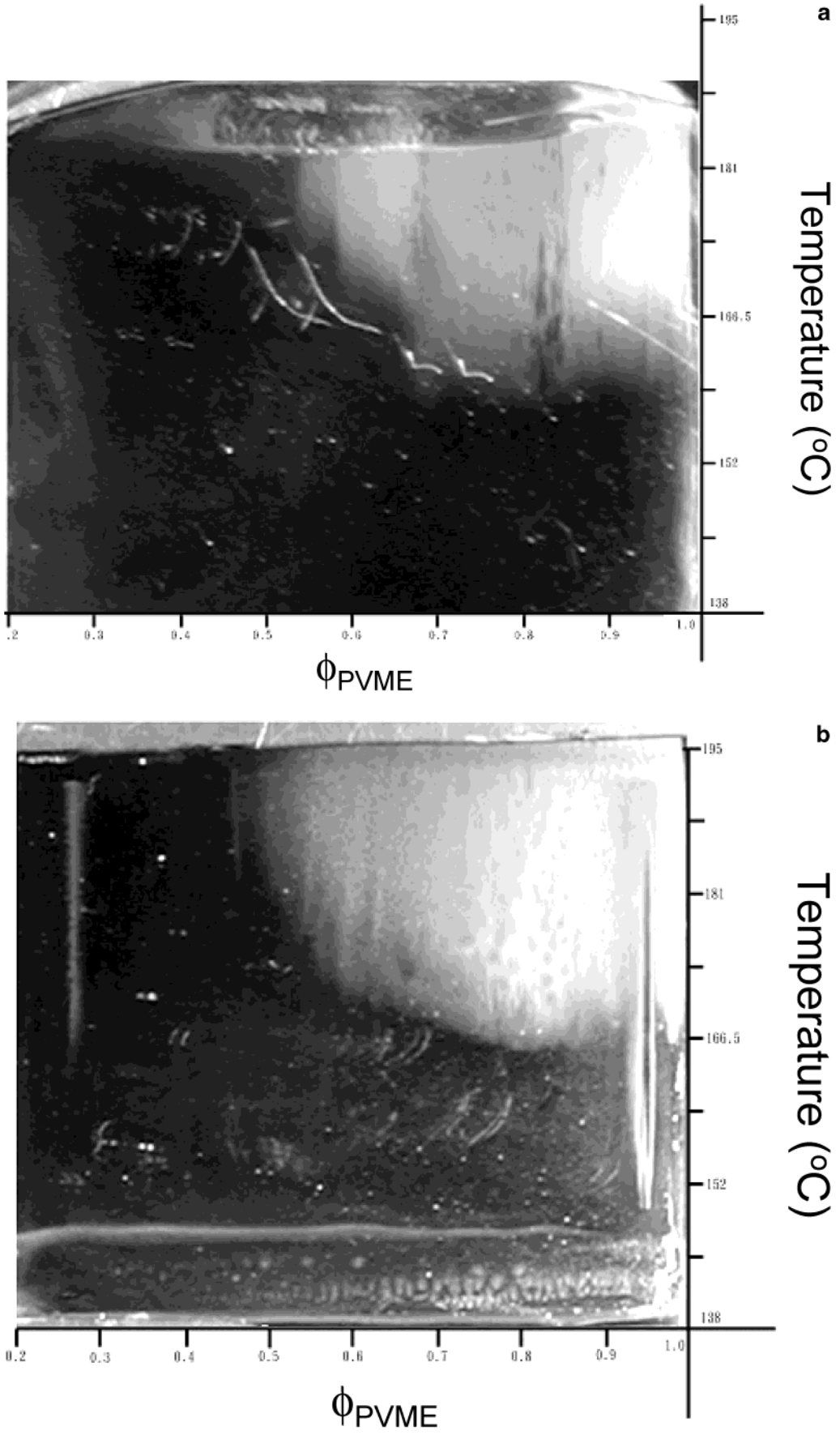

Figure 5. Combinatorial phase diagrams for the unfilled dPS/PVME blend (a**)** and for the dPS/PVME blend with a 2C18M volume fraction of 0.008 **(**b**)**. Phase-separated areas appear cloudy due to the refractive index contrast between the dPS-rich and the PVME-rich domains. The phase boundary is sharper in the case of the filled blend film. Average standard uncertainties in temperature and polystyrene mass fraction have been determined previously for these measurements to be ±1.5 °C and ±0.006, respectively [25] and are much smaller than the expected shifts in the phase diagram.

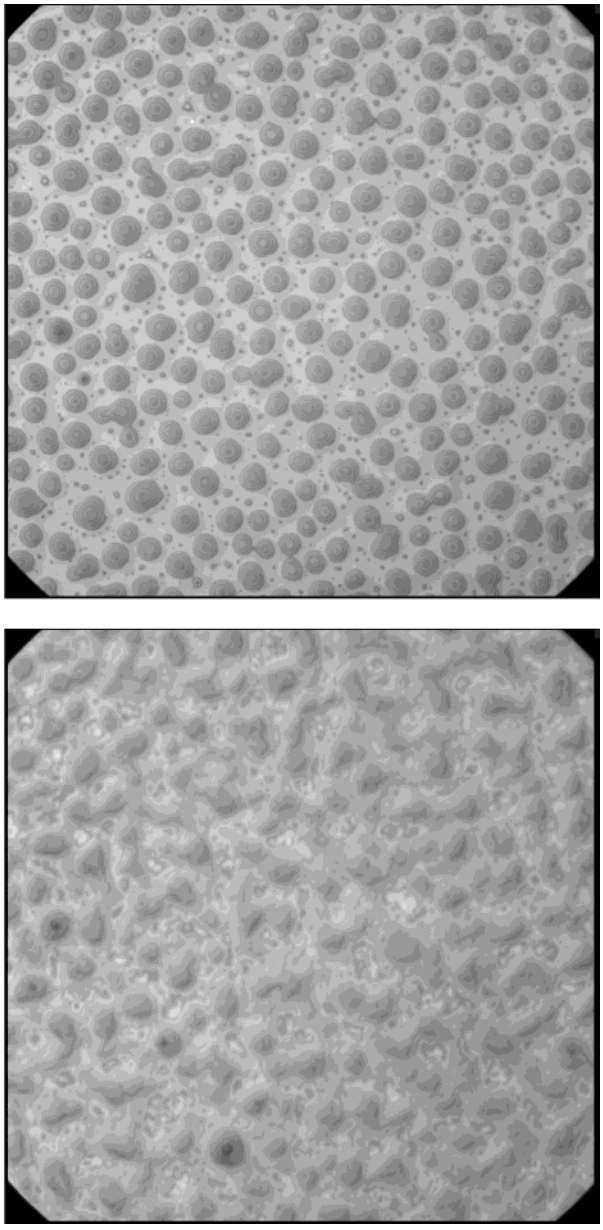

Figure 6. Optical micrograph of the two-phase region from the unfilled dPS/PVME blend film shown in Figure 6a (a**)** and from the two-phase region from the dPS/PVME nanocomposite film shown in Figure 6b **(**b**)** acquired with a 100× objective lens, resulting in 150 × 150 μm images. In the unfilled film, the concentric refraction rings identify the circular domains as dewet holes.

ary. However, these effects cannot also be separated from the film stabilization by the addition of nanoparticles. Nevertheless, the presence of the nanofillers, as illustrated by 100× magnification optical microscopy images taken of the cloudy regions of the same samples (Figure 5a,b) and shown in Figure 6a,b, results in increased stabilization of the thin film. Figure 6a for the unfilled blend clearly reveals the diffraction rings characteristic of a dewet film. On the other hand, the cloudy region in the layered silicate containing film merely consists of a spinodal phase separated structure. Such stabilization of filled polymer films has been previously observed for systems where the polymer and the filler have favorable interactions.[34]

The phase behavior of dPS−PVME blends, quite unexpectedly, appears to be essentially unaltered by the addition of organically modified montmorillonite, with detailed phase diagrams and Flory−Huggins interaction parameters being largely unaffected by such addition. In such nanocomposites with a large surface area per unit volume, it is anticipated that preferential polymer−organically modified silicate interactions and polymer confinement could affect the phase behavior. Confinement effects would be expected to increase the compatibility of the components: surface segregation or wetting of one of the components leads to near-surface off-critical concentrations even for films with an overall critical concentration and therefore to apparent increased stability.[7,35] Preferential attractions, on the other hand, would be expected to lead to destabilization of the blend.[9,36]

In these nanocomposites, two types of confinement need to be considered—the confinement on the order of 2−3 nm between silicate sheets stacked as intercalated tactoids and confinement between silicate tactoids with length scales on the order of 100−1000 nm depending on the silicate concentration and effective dispersion (as shown below). For the nanocomposites considered here, even the largest volume fraction of the nanofiller employed is small (a volume fraction of 0.04), so only a small minority (a volume fraction of <0.05) of the polymer chains are intercalated, and the effects of the intercalation (and extreme confinement) are small. On the other hand, the average tactoid center-to-center distance d (in nm), calculated assuming a layer−layer distance of 3 nm and an effective layer diameter of 0.5 μm, is

$$d \sim 80\left(\frac{n}{\phi_{LS}}\right)^{1/3} \tag{6}$$

where n is the number of silicate layers in a tactoid and ϕ_{LS} is the volume fraction of layered silicate. The distance between silicate tactoids consisting of five layers ($n = 5$)[25,27] ranges from 300 to 1000 nm for ϕ_{LS} ranging from 0.04 to 0.004. Previous studies indicate that for PS−PVME blends confined on a Si/SiO_2 surface lead to stabilization of the single phase with the minimum thickness for such an effect to be manifested being ≈100 nm. Thus, based on this simple calculation we anticipate that confinement of the polymer blend between the silicate tactoids would not contribute significantly to the stabilization or destabilization of the polymer blend.

On the other hand, as noted in the Introduction, PVME is significantly more polar than PS and it is thus anticipated that the PVME would strongly interact with the silicate layers and alter the phase behavior of the PS−PVME blend. We note parenthetically (as demonstrated in the accompanying paper) that the layered silicates are found more frequently in the PVME-rich phase in phase-separated morphologies. The stronger PVME layered silicate interaction could also be manifested in the microstructure of the nanocomposite, i.e., delamination of the silicate tactoids or formation poorly ordered intercalated nanocomposites. The XRD spectra for 2C18M and nanocomposites of dPS and PVME and the blend of dPS and PVME with 2C18M are shown in Figure 7. Surprisingly, in all cases only an intercalated nanocomposite was obtained. The (001) reflection, corresponding to the center−center distance between the silicate layers, is shifted to lower diffraction angles for the nanocomposites and indicates that the layered structure of the silicate sheets is preserved after infil-

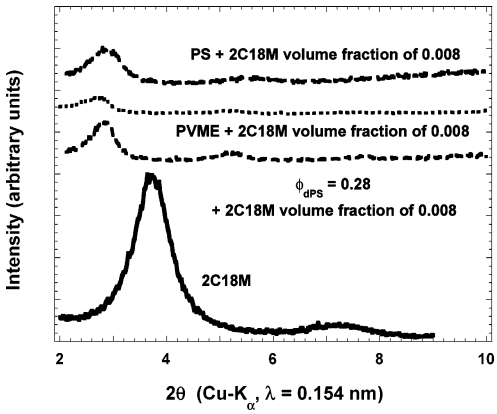

Figure 7. XRD spectra for the pure 2C18M, and for its nanocomposites with dPS, PVME, and the $\phi_{dPS} = 0.28$ blend. Note that the (001) reflection is at a lower angle for all nanocomposites, indicating intercalation by both dPS and PVME.

tration by the polymers, albeit with an expanded gallery. The extent of layer−layer order is essentially unaffected by the addition or choice of polymer on the basis of the (001) peak width and the development of higher order reflections in the diffraction spectra.[4,37] The layer center-to-center spacing is determined from the angular location of the (001) reflection (θ_{001}) using Bragg's Law:

$$d_{001} = \frac{\lambda}{2\sin(\theta_{001})} \tag{7}$$

The intergallery height (h) is then calculated by subtracting the thickness of a single silicate layer (≈9.5 Å) from d_{001}. The value of h for 2C18M is 13.5 Å, while those for the dPS, PVME, and dPS−PVME blend nanocomposites are 21.5, 22, and 22 Å respectively. While the structure of the nanocomposites with PVME are unaffected, this only implies that the strength of the PVME layered silicate interaction is not dramatically different from that of PS and the layered silicates. This might result from the coverage of the surface by the charge balancing alkyl cations that are less compatible with PVME than with PS. Thus, in the absence of anticipated strong stabilizing and/or destabilizing influences, the phase behavior of the PS−PVME blend system is essentially unaffected by the addition of the nanoparticles. Nevertheless, the kinetics and morphological development of phase separation are significantly influenced by the addition of these nanoparticles and are described in a previous paper.[38]

Concluding Remarks

SANS and a two-dimensional concentration and temperature gradient based combinatorial method demonstrate that the presence of 2C18M up to a volume fraction of 0.008 does not significantly alter the LCST phase diagram of a binary blend of dPS and PVME. Analysis of the SANS data in the context of the incompressible RPA reveals that while at temperatures far below the LCST the χ values depend on the concentration of added layered silicate, at temperatures close to the LCST, where concentration fluctuations are large, the thermodynamics are not significantly affected by the presence of the layered silicate. These results are explained by the lack of a strong preferentiality for either of the blend components by the silicate surfaces, as implied by the XRD measurements, which show only intercalation of 2C18M by both components. Issues such as confinement between silicate layers and between silicate tactoids appear not to have a significant impact on the phase behavior in these nanocomposite materials. Thus, these systems provide a reasonable starting point to investigate the influence of such nanoscale layered materials on the phase separated morphology and kinetics of phase separation, examined in the accompanying paper.

Acknowledgment. We thank Dr. Barry Bauer for generously donating the PVME and Dr. Amit Sehgal, Prof. Carson Meredith, and Dr. Archie P. Smith for their help with the combinatorial experiments. We (K.Y. and R.K.) would also like to thank the National Science Foundation (DMR-9875321) and NIST for funding this research. The SANS measurements conducted at NIST were supported by the National Science Foundation under Agreement No. DMR-9986442. This work made use of TCSUH/MRSEC Shared Facilities supported by the State of Texas through TCSUH and by NSF (DMR-9632667).

References and Notes

(1) Enikolopyan, N. S., Ed. *Filled Polymers I: Science and Technology*; Springer-Verlag: Berlin; New York, 1990; Vol. 96.
(2) Theng, B. K. G. *Formation and Properties of Clay-Polymer Complexes*; Elsevier Scientific Publishing Company: New York, 1979; Vol. 9.
(3) Kojima, Y.; Usuki, A.; Kawasumi, M.; Okada, A.; Kurauchi, T.; Kamigaito, O. *J. Polym. Sci. Part A: Polym. Chem.* **1993**, *31*, 983−986. Usuki, A.; Kojima, Y.; Kawasumi, M.; Okada, A.; Fukushima, Y.; Kurauchi, T.; Kamigaito, O. *J. Mater. Res.* **1993**, *8*, 1179−1184.
(4) Giannelis, E. P.; Krishnamoorti, R.; Manias, E. *Adv. Polym. Sci.* **1999**, *138*, 107−147. Krishnamoorti, R.; Vaia, R. A.; Giannelis, E. P. *Chem. Mater.* **1996**, *8*, 1728.
(5) Giannelis, E. P. *Adv. Mater.* **1996**, *8*, 29−35.
(6) Jain, A.; Gutmann, J. S.; Garcia, C. B. W.; Zhang, Y. M.; Tate, M. W.; Gruner, S. M.; Wiesner, U. *Macromolecules* **2002**, *35*, 4862−4865.
(7) Binder, K. In *Advances in Polymer Science*; Granick, S., Ed.; Springer: Heidelberg, 1999; Vol. 138, pp 1−90.
(8) Chen, H. In *Department of Materials Science and Engineering*; Cornell University: Ithaca, NY, 2001.
(9) Lee, K. M.; Han, C. D. *Macromolecules* **2003**, *36*, 804−815.
(10) Gelfer, M. Y.; Sung, H. H.; Liu, L.; Hsiao, B. S.; Chu, B.; Rafailovich, M. H.; Si, M.; Zaitsev, V. *J. Polym. Sci., Part B: Polym. Phys.* **2003**, *41*, 44−54. Voulgaris, D.; Petridis, D. *Polymer* **2002**, *43*, 2213−2218.
(11) Ben Cheikh Larbi, F.; Leloup, S.; Halary, J. L.; Monnerie, L. *Polym. Commun.* **1986**, *27*, 23−25. Yang, H.; Hadziioannou, G.; Stein, R. S. *J. Polym. Sci.: Polym. Phys. Ed.* **1983**, *21*, 159−162.
(12) Shibayama, M.; Yang, H.; Stein, R. S.; Han, C. C. *Macromolecules* **1985**, *18*, 2179−2187.
(13) Schwahn, D.; Mortensen, K.; Springer, T.; Yee-Madeira, H.; Thomas, R. *J. Chem. Phys.* **1987**, *87*, 6078−6087.
(14) Choi, S.; Liu, X.; Briber, R. M. *J. Polym. Sci., Part B: Polym. Phys.* **1998**, *36*, 1−9.
(15) Vaia, R. A.; Giannelis, E. P. *Macromolecules* **1997**, *30*, 8000−8008; Vaia, R. A.; Giannelis, E. P. *Macromolecules* **1997**, *30*, 7990−7999.
(16) Giese, R. F.; Van Oss, C. J. *Journal Dispersion Sci. Technol.* **1998**, *19*, 775−783. Norris, J.; Giese, R. F.; Van Oss, C. J.; Costanzo, P. M. *Clays Clay Miner.* **1992**, *40*, 327−334. Van Oss, C. J.; Giese, R. F. *Clays Clay Miner.* **1995**, *43*, 474−477.
(17) Della Volpe, C.; Siboni, S. *J. Adhesion Sci. Technol.* **2000**, *11*, 235−272. Van Oss, C. J.; Chaudhury, M. K.; Good, R. J. *Separation Sci. Technol.* **1989**, *24*, 15−30. Wu, W.; Giese, R. F.; Van Oss, C. J. *Langmuir* **1995**, *11*, 379−382.

(18) Brandrupt, J., Immergut, E. H., Grulke, E. A., Eds. *Polymer Handbook*, 4th ed.; Wiley-Interscience: New York, 1999.
(19) Certain equipment and instruments or materials are identified in the paper in order to adequately specify the experimental details. Such identification does not imply recommendation by the National Institute of Standards and Technology, nor does it imply the materials are necessarily the best available for the purpose.
(20) According to ISO 31-8, the term molecular weight has been replaced by "relative molecular mass" M_r. Thus, if this nomenclature and notation were to be followed in this publication, one would write $M_{r,w}$ instead of the historically conventional M_w for the weight-average molecular weight, with similar changes for M_n, and it would be called the "weight average relative molecular mass". The older, more conventional notation, rather than the ISO notation, has been employed for this publication.
(21) Krishnamoorti, R.; Ren, J.; Silva, A. S. *J. Chem. Phys.* **2001**, *114*, 4968−4973.
(22) Ren, J.; Silva, A. S.; Krishnamoorti, R. *Macromolecules* **2000**, *33*, 3739−3746.
(23) Krishnamoorti, R.; Silva, A. S.; Mitchell, C. A. *J. Chem. Phys.* **2001**, *115*, 7175−7181.
(24) Silva, A. S.; Mitchell, C. A.; Tse, M. F.; Wang, H.-C.; Krishnamoorti, R. *J. Chem. Phys.* **2001**, *115*, 7166−7174.
(25) Meredith, C. J.; Karim, A.; Amis, E. J. *Macromolecules* **2000**, *33*, 5760−5762.
(26) Meredith, C. J.; Smith, A. P.; Karim, A.; Amis, E. J. *Macromolecules* **2000**, *33*, 9747−9756.
(27) Tanaka, K.; Yoon, J.-S.; Takahara, A.; Kajiyama, T. *Macromolecules* **1995**, *28*, 934−938.
(28) Ubrich, J. M.; Ben Cheikh Larbi, F.; Halary, J. L.; Monnerie, L.; Bauer, B. J.; Han, C. C. *Macromolecules* **1986**, *19*, 810−815.
(29) Ho, D. L.; Briber, R. M.; Glinka, C. J. *Chem. Mater.* **2001**, *13*, 1923−1931.
(30) Hanley, H. J. M.; Muzny, C. D.; Ho, D. L.; Glinka, C. J.; Manias, E. *Int. J. Thermophys.* **2001**, *22*, 1435−1448.
(31) Krishnamoorti, R., unpublished data.
(32) Stein, R. S.; Hadziioannou, G. *Macromolecules* **1984**, *17*, 1059.
(33) The filled $\phi_{dPS} = 0.18$ blend could not be measured because of degradation during the sealing of the tube and the easy degradation of PVME in the presence of the layered silicates.
(34) Sharma, S.; Rafailovich, M. H.; Peiffer, D.; Sokolov, J. *Nano Lett.* **2001**, *10*, 511−514. Limary, R.; Swinnea, S.; Green, P. F. *Macromolecules* **2000**, *33*, 5227−5234. Barnes, K. A.; Karim, A.; Douglas, J. F.; Nakatani, A. I.; Gruell, H.; Amis, E. J. *Macromolecules* **2000**, *33*, 4177−4185.
(35) Karim, A.; Slawecki, T. M.; Kumar, S. K.; Douglas, J. F.; Satija, S. K.; Han, C. C.; Russell, T. P.; Liu, Y.; Overney, R.; Sokolov, O.; Rafailovich, M. H. *Macromolecules* **1998**, *31*, 857−862. Krausch, G.; Dai, C. A.; Kramer, E. J.; Bates, F. S. *Ber. Bunsen-Ges. Phys. Chem. Chem. Phys.* **1994**, *98*, 446−448. Jones, R. A. L.; Norton, L. J.; Kramer, E. J.; Bates, F. S.; Wiltzius, P. *Phys. Rev. Lett.* **1991**, *66*, 1326−1329.
(36) Douglas, J. F., personal communication.
(37) Manias, E.; Chen, H.; Krishnamoorti, R.; Genzer, J.; Kramer, E. J.; Giannelis, E. P. *Macromolecules* **2000**, *33*, 7955−7966.
(38) Yurekli, K.; Karim, A.; Amis, E. J.; Krishnamoorti, R. *Macromolecules* **2003**, *36*, 7256−7267.

MA0302098